Proceedings of The Twelfth (2002) International Offshore and Polar Engineering Conference
Kitakyushu, Japan, May 26−31, 2002

ISBN 1-880653-58-3 (Set); ISSN 1098-6189 (Set)

Coupling Hydrodynamic and Aerodynamic Computations to Predict Sailing Boat Behaviour

J.P. Boin[1], *M. Guilbaud*[1] *and M. Ba*[2]
Laboratoire d'Etudes Aérodynamiques
(UMR CNRS n°6609)
[1]CEAT-University of Poitiers,
[2]ENSMA, Poitiers, France

Y. Roux
Laboratoire de Mécanique, University of
Le Havre,
Le Havre, France

F. Hauville
Institut de Recherche de l'Ecole
Navale, Ecole Navale et GFP,
Brest, France

ABSTRACT

We present the coupling of two computing codes for the hull hydrodynamics and the sail aerodynamics to predict the performance of a sailing boat. The first one is a Boundary Element Method one using a Green's function (steady wave resistance or diffraction-radiation with forward speed). The aerodynamic code is based on a lifting surface model for the sails and a particle method for its wake. The motion of the sailing boat upward is studied by computing the acceleration at each time step and then deducing the velocity and position of the boat. Results are presented only in steady flow.

KEY WORDS: Hydrodynamics; Aerodynamics; Sailing boat; Wave resistance; Green function; Boundary Element Method.

INTRODUCTION

The progress of numerical codes to compute both the aerodynamics of sails and the hydrodynamic flows about hulls enables today to develop a numerical tool to be used in the design of sailing boats. We present recent results concerning the numerical simulation of a navigating sailing boat. This simulation is done by the coupling of a hydrodynamic computer code and of an aerodynamic one. The hydrodynamic computations are performed by a velocity based frst order panel method, using either the wave resistance Green function or the diffraction-radiation with forward speed one in the frequency domain. When compared with Rankine method using the elementary solution of the Laplace equations in an unbounded fluid (see Sclavounos, 1996 for a review), the advantages of Kelvin singularities using the Green function satisfying a linearized form of the free surface boundary condition are to satisfy also the radiation condition automatically. Furthermore, only a grid on the body is needed, leading to smaller systems of equations to solve and avoiding any wave reflection on the boundary of the free surface grid or some filtering of the smaller wavelengths as in the Rankine methods. To compute accurately the integrals on the hull panels or on waterline segments involving the Green function or its derivatives appearing in the third Green identity, the boundary and Fourier integrals have been interchanged. The first ones are calculated analytically and the second ones by a Simpson method of integration with a variable step. The accuracy of these integrations, presented in a preliminary version by Boin *et al.* (2000), have been checked in Ba *et al.* (2001a,b) by comparing the results obtained by a steepest descent method to compute the Green function, Brument and Delhommeau (1997), Brument (1998) or Maury (2001). The unsteady aerodynamic simulation is based on a description of the flow by means of lifting surfaces for the sails and particle method for its wake. At each time step, particles are created along given lines (the trailing edge of the sail) in order to satisfy a condition formally derived from the Joukowsky condition. The velocity field of the particles is computed by the Biot-Savart relation and the deformation term is obtained through an integral relation by differentiating the Biot-Savart law.

In this paper, we consider the motion of a boat sailing upwind (the angle of incidence remains less than 70° from the true wind direction) to keep the flow attached on the sail. At each time step, forces on the sails are computed and from the knowledge of the hull's position, the forces on the hull are calculated. The acceleration is estimated by the solution of the Newton's equation. The velocity and the position of the boat are estimated from the acceleration by the Adam Bashforth integration scheme. Examples of results obtained for a First class 8 sailing boat in steady flow are presented.

NUMERICAL METHODS

Hydrodynamic flow

Consider a ship advancing in waves or in a quiet ocean along a straight path with constant velocity U in water of effectively infinite depth and lateral extent. The flow is observed from a Cartesian system of co-ordinates moving with the ship. The x axis is taken along the path of the ship and points toward the ship bow (i.e. the ship advancing in the direction of the positive x axis). The z axis is vertical and points upward; the mean free surface is the plane z=0. Based on the assumptions of perfect fluid, irrotational flow and small wave steepness, the velocity potential can be written as the sum of a basic (steady) and a time harmonic (unsteady) $f(x,y,z)e^{iwt}$ potentials. Calling f either the steady velocity potential or its spatial part, they must satisfy the Laplace equation into the fluid, the body condition on the body S:

$$\frac{\partial f}{\partial n} = \left(\vec{V}_{rel}\right)\cdot \vec{n} \quad \text{with } \vec{V}_{rel} = \vec{U}_{\infty} \text{(steadyflow)}$$
$$\text{or } \vec{V}_{rel} = \vec{V} + \vec{\Omega} \wedge \vec{n} \text{ (unsteady flow)} \tag{1}$$

where $\vec{U}_{\infty}$, $\vec{V}$ and $\vec{\Omega}$ are respectively the free-stream velocity, the translation and rotation velocities of the body if any, and the linearized free-surface boundary condition on the mean free-surface S_F (z=0):

$$\left(iw + U_{\infty}\frac{\partial}{\partial x}\right)^2 f + g\frac{\partial f}{\partial x} = 0 \quad on \; z = 0 \tag{2}$$

plus the radiation condition and the condition at infinity. w is the circular frequency.

By use of the Green's third identity for a computational closed domain limited by the body surface S, the free surface S_F and the surface of a half sphere located at infinity S_∞, the velocity potential f can be written under the form:

$$C(x,y,z)f(x,y,z) = \iint_{S+S_F+S_\infty}\left(G\frac{\partial f}{\partial n} - f\frac{\partial G}{\partial n}\right)ds \tag{3}$$

In Eq. 3, G is either the wave resistance or the radiation-diffraction with forward speed Green function satisfying the same conditions as f, except the body one. Details on these Green's functions can be found in Ponizy *et al*. (1998) or in Ba and Guilbaud (1995). With the previous assumptions and by transforming the boundary integral on the free surface into a contour one on the waterline C_L using the Stokes theorem, Eq. 3 for f on *S* is transformed into:

$$C(x,y,z)f(x,y,z) = \iint_S\left(G\frac{\partial f}{\partial n} - f\frac{\partial G}{\partial n}\right)ds - F\int_{C_L}\left[2i\tilde{w}fG + F\left(G\frac{\partial f}{\partial x'} - f\frac{\partial G}{\partial x'}\right)\right]dy' \tag{4}$$

where $\tilde{w} = w\sqrt{L/g}$ is the non-dimensional circular frequency. Steady flows deal with lifting problems using a mixed distribution of sources and doublets but in the present version, unsteady computations are restricted only to non lifting problem, using only source distribution. By applying the $\partial/\partial n$ operator to the previous equation, an integral equation enabling to compute the unknown distribution can be obtained using the body condition, Eq. 1. In the steady case, the sources are distributed on the hull; doublets are distributed on the hull plane of symmetry and on semi-infinite strips extending from the trailing edge of the lifting parts of the hull with a constant intensity equal to the value at the trailing edge, instead of being oscillating as in harmonic flows). The body condition can be written as:

$$\forall M \in S \quad \frac{\tilde{s}(M)}{2} - \frac{1}{4p}\iint_S \tilde{s}(M')\frac{\partial \tilde{G}}{\partial n_M}dS_{M'}$$
$$+\frac{U_\infty^2}{4p\,g}\int_C \tilde{s}(M')\frac{\partial \tilde{G}}{\partial n_M}(\vec{n}_{M'}.\vec{x})dy_{M'} - \frac{1}{4p}\iint_{\Sigma\cup\Sigma_B}\tilde{m}(M')\frac{\partial^2 \tilde{G}}{\partial n_M \partial n_{M'}}dS_{M'} = \frac{\partial \tilde{\Phi}}{\partial n_M} \tag{5}$$

Then, potential, pressure forces and wave elevation can be calculated.
For the numerical resolution, the hull surface is divided into n_c columns of n_p panels giving $N = n_b \cdot n_p$ panels on the whole body. Consequently, the waterline is also divided into n_p segments. The doublets are distributed on $N/2$ panels on the plane of symmetry and n_c strips in the wake. In the present method, each data is assumed to be constant on each panel or waterline segment. The integral equation can be then transformed into a set of linear equations obtained by writing the body condition on each panel and eventually a Kutta condition on the trailing edge of the lifting parts of the body. The values of the unknowns, source or doublet, on the waterline segments are assumed to be equal to their values on the dosest panel. To compute the coefficients in the previous system, it is necessary to compute the following integrals given in Eq. 6 by boundary (on a elementary panel or strips) or line (on a waterline segment) integrals on the Green function, on the first derivatives and even second ones if lifting effects are to be taken into account:

$$J_1 = \iint_{Sj} G_{ij}\,ds;\; J_2 = \iint_{Sj}\frac{\partial G_{ij}}{\partial n_{M'}}ds;\; J_3 = \iint_{Sj}\frac{\partial^2 G_{ij}}{\partial n_{M'}\partial n_M}ds;$$
$$J_4 = \int_{C_l} G_{ij}\,ds;\; J_5 = \int_{C_l}\frac{\partial G_{ij}}{\partial n_{M'}}ds;\; J_6 = \int_{C_l}\frac{\partial^2 G_{ij}}{\partial n_{M'}\partial n_M}ds \tag{6}$$

The Green functions are computed using a single integral formula involving the complex exponential integral function. The Fourier integration in the θ-space is calculated as in Nontakaew *et al*. (1997) by an adaptive quadrature method (as proposed by Lyness, 1970 or Malcom and Simpson, 1975), where the integration step decreases as the integrand becomes more oscillating. Each interval is divided into 2 equal sub-intervals and the integral on the whole interval and the sum of the 2 integrals on the 2 sub ones, each computed with a 5 points Simpson method, are compared to reach a prescribed error. The procedure is pursued till convergence. The error on the whole domain and the corresponding error on one of the sub-domain can be related, Guttman (1983). This method reduces the CPU times and gives accurate results for any values of the parameters.
So, in Eq. 5, it is necessary to compute accurately the integrals on panels or waterline segments of Eq 6 involving the Green function or its derivatives. For the boundary integrals, the integrals are computed after having interchanged the boundary integrals and the θ-ones, the former being obtained by an analytical integration based on the Stokes theorem transforming the surface integrals on contour of the panel, following Bougis (1981):

$$I = \iint_S \frac{d^2 f}{dz^2}ds = \sum_{k=1}^{m} A_k \frac{f(z_{k+1}) - f(z_k)}{z_{k+1} - z_k} \tag{7}$$

The Rankine terms of the Green function, often studied in aerodynamics or hydrodynamics using Rankine's singularities, will not be considered here and are computed analytically too. For a panel close to the free surface or a waterline segment and a field point very close to the free-surface some numerical difficulties arise but this particular situation arise only for computations of the free surface elevation.

Aerodynamic of the sails

Flow modeling is based on the vortex element method (VEM). This method is suitable for external flows for bounded vorticity support. It is the case for lifting surfaces, where the turbulent shear flow along the surface and the wake formed by the vortex shedding along the trailing edge are represented by dipole surface distribution and vortex sheets, respectively. During the last ten years, this method was successfully validated, particularly to capture dynamic wake effects in details (Charvet and Huberson, 1992; Charvet *et al*., 1996; Breard *et al*., 1997).

This method is basically made of two parts : a lifting body problem and a wake problem. These two problems are coupled by means of a kind of Kutta condition that has been derived from the kinematic and dynamic conditions along the separation lines. Usually, these lines are reduced to the trailing edges although more complicated situations have sometimes been considered. Except when writing this Kutta condition, the flow has been assumed to be inviscid. The lifting problem is solved by means of a boundary integral method : the surface of the body is represented using panels of rectangular shape which are used to satisfy the potential slip conditions. Specifically, a dipole strength was associated with each panel, and the strength of the dipole was adjusted by imposing that the normal velocity component at the surface of the body must vanish at control points (c.f. Fig.1; Eqs. 11~12). The wake has been modeled by means of the particle method itself (c.f. Rehbach, 1977). According to this method, the vorticity distribution within the wake is described by means of particles carrying vortices. The motion of particles is computed in a Lagragian framework. The vorticity on each particle has to satisfy the Helmholtz equation.

According to the Helmholtz's decomposition theorem, the velocity field is given by:

$$\vec{U} = \vec{U}_\infty + \vec{U}_w + \vec{U}_f + \vec{U}_{ext} \tag{8}$$

where $\vec{U}_\infty$ represents the inflow velocity, $\vec{U}_f$ is derived from a scalar potential f, and $\vec{U}_w$ **,** is derived from a potential vector $\vec{y}$ **,** representing respectively the body's influence and the wake's influence, $\vec{U}_{ext}$ is the velocity field induced for example by an another lifting body with its wake.

The Euler equations in velocity-vorticity formulation for particle i are expressed in Lagrangian coordinates. $\vec{X}_i$ is a point which can be the geometric center of the particle, the baricentric centre for the vorticity contained in the particle or any other point representative of the particle location and $\vec{\Omega}_i$ their circulation which is the amount of vorticity initially contained in the particle:

$$\vec{\Omega}_i = \iiint_{P_i} \vec{w}\, ds \; ; \quad \vec{\Omega}_i \wedge \vec{X}_i = \iiint_{P_i} \vec{w} \wedge \vec{x}\, ds \; . \tag{9}$$

where $\vec{w}$ is the absolute vorticity.

The evolution equation for $\vec{X}_i$, $\vec{\Omega}_i$ are:

$$\begin{cases} \dfrac{D\vec{X}_i}{Dt} = \vec{U}_\infty + \vec{U}_w + \vec{U}_f + \vec{U}_{ext}\left(\vec{X}_i, t\right) \\ \dfrac{D\vec{\Omega}_i}{Dt} = -\dfrac{1}{4p} \displaystyle\sum_{p=1(\neq i)}^{N_j + N_p(t)} \left(\frac{3}{\left|\vec{X}_p - \vec{X}_i\right|^5} \left(\vec{X}_p - \vec{X}_i\right) \left(\vec{\Omega}_i \cdot \left(\vec{\Omega}_p \wedge \left(\vec{X}_p - \vec{X}_i\right)\right)\right) \right. \\ \qquad\qquad \left. + \dfrac{1}{\left|\vec{X}_p - \vec{X}_i\right|^3} \left(\vec{\Omega}_p \wedge \vec{\Omega}_i\right) \right) \\ \qquad + \left(\vec{\Omega}_i \cdot \overline{\overline{grad}}\right)\left(\vec{U}_\infty + \vec{U}_{ext}\right)\left(\vec{X}_i, t\right) + n\Delta\vec{\Omega}_i \end{cases} \tag{10}$$

Let N_j be the number of bound vortex particles equivalent to the dipoles (Hess, 1969), $N_p(t)$ the number of free vortex particles and N_f the number of panels:

$$\vec{U}_w\left(\vec{X}_i, t\right) = -\frac{1}{4p} \sum_{p=1(\neq i)}^{N_p(t)} \frac{\vec{\Omega}_p\left(t\right) \wedge \left(\vec{X}_p - \vec{X}_i\right)}{\left|\vec{X}_p - \vec{X}_i\right|^3}; \tag{11}$$

$$\vec{U}_f\left(\vec{X}_i, t\right) = -\frac{1}{4p} \sum_{p=1(\neq i)}^{N_f} m_p\left(t\right) \sum_{n=1}^{4} \vec{U}_{ip}^{\,n} \text{ (cf. fig. 1)}$$

$$\vec{U}_{ip}^{\,n} = \frac{\vec{r}_{ip}^{\,n_1} \wedge \vec{r}_{ip}^{\,n_2}}{\left|\vec{r}_{ip}^{\,n_1} \wedge \vec{r}_{ip}^{\,n_2}\right|^2} \left[\left|\vec{r}_{ip}^{\,n_1}\right| + \left|\vec{r}_{ip}^{\,n_2}\right|\right] \left[1 - \frac{\vec{r}_{ip}^{\,n_1} \cdot \vec{r}_{ip}^{\,n_2}}{\left|\vec{r}_{ip}^{\,n_1}\right| \left|\vec{r}_{ip}^{\,n_2}\right|}\right] \tag{12}$$

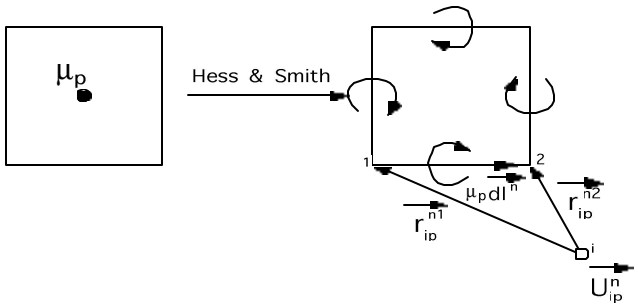

Fig. 1 Dipole-vortex equivalence

The dipole distribution m on the surface of the body, which is used to compute $\vec{U}_f$, has been set in order to satisfy the non-penetration condition. It is obtained by solving the full matrix linear system:

$$[A][m] = [S] \tag{13}$$

where [m] is the unknown vector of the system, [S] the known vector of boundary conditions $\left(-\left[\vec{U}_\infty + \vec{U}_w + \vec{U}_{ext}\right] \cdot \vec{n}\right)$ and [A] a square matrix called "influence matrix". Matrix [A] depends only on the body geometry. The a_{ij} term of this matrix represents the influence of the unknown m_j on the boundary term S_i. It is obtained by computing the normal velocity induced by a unit dipole strength m_j at the control point of panel i:

$$a_{ij} = \frac{\vec{n}_i}{4p} \sum_{n=1}^{4} \vec{U}_{ij}^{\,n} \qquad \text{(c.f. Eq. 12)} \tag{14}$$

The singular behaviour of these equations when $\vec{X}_p$ tends to $\vec{X}_i$ leads to the introduction of a regularisation function. Thus, we have replaced the singular kernel (c.f. Eq. 12) by the convolution product of this kernel by the function f which is defined by:

$$f\left(r\right) = \frac{r^3}{\left(1 + r^6\right)^{1/2}}$$

We set for the desingularised Biot-Savart law:

$$\vec{U}_w\left(\vec{X}_i,t\right)=-\frac{1}{4p}\sum_{p=1(p\neq i)}^{N_p(t)} f\left(\frac{\vec{X}_p-\vec{X}_i}{d_i}\right)\frac{\vec{\Omega}_p(t)\wedge\left(\vec{X}_p-\vec{X}_i\right)}{\left|\vec{X}_p-\vec{X}_i\right|^3} \qquad (15)$$
$$=-\frac{1}{4p}\sum_{p=1}^{N_p(t)}\frac{\vec{\Omega}_p(t)\wedge\left(\vec{X}_p-\vec{X}_i\right)}{\left(\left(\vec{X}_p-\vec{X}_i\right)^6+d_i^6\right)^{\frac{1}{2}}}$$

where d_i is the distance with respect to the singularity, from which the regularisation is done.
The amount of vorticity initially contained in the particle is obtained by application of the Bernoulli relation on the separation line (with $\vec{U}_{te}=\frac{1}{2}\left(\vec{U}^+ +\vec{U}^-\right)$, the trailing edge velocity):

$$\frac{\partial m}{\partial t}+\vec{U}_{te}\cdot\overrightarrow{grad}m=0$$

So, during one step time *dt*, we evaluate the location and the vorticity of the new vortex particle by the following equations:

$$\vec{\Omega}_i=\left[dl_i\left(m_i\left(t+\Delta t\right)-m_i\left(t\right)\right)\right]\vec{i}+\left[\Delta t\left|\vec{U}_{te}\right|\frac{m_{i+1}-m_{i-1}}{2}\right]\vec{j} \qquad (16)$$
$$\vec{X}_i=\vec{X}_{te}+\vec{U}_{te}\frac{\Delta t}{2}$$

$\left(\vec{X}_{te},\vec{i},\vec{j},\vec{n}_i\right)$ is the local frame of reference with $\vec{n}_i$ the unit normal vector on panel *i* and $\vec{i}$ the tangent vector on the trailing edge. dl_i is the length of the side of panel *i* which is a part of the trailing edge.
For more generality, we consider two Cartesian frames of reference, the first one is fixed (inertial frame), and the other one moving relative to the first with the translation velocity $\vec{V}_0$ and the angular velocity $\vec{\Phi}$:

$$\vec{U}_e\left(M\right)=\vec{V}_0\left(O\right)+\vec{\Phi}\wedge\overrightarrow{OM}$$

The relation between the velocity $\vec{U}_a\left(M\right)$ of a fluid particle in the absolute frame of reference and its relative velocity $\vec{U}_r\left(M\right)$ in the moving frame is:

$$\vec{U}_r\left(M\right)=\vec{U}_a\left(M\right)-\vec{U}_e\left(M\right)$$

The non penetration condition takes into account the relative velocity. We have the same linear system that Eq. 13 with the new known vector of boundary conditions:

$$S(t)=-\left(\vec{U}_\infty\left(t\right)+\vec{U}_w\left(t\right)+\vec{U}_{ext}\left(t\right)-\vec{U}_e\left(t\right)\right)\cdot\vec{n}$$

The vorticity creation model which established the link between the solid walls discretisation and the particle wake is the same, taking into account the body motion $\vec{U}_e\left(M\right)$:

$$\vec{\Omega}_{ia}=\left[dl_i\left(m_i\left(t+\Delta t\right)-m_i\left(t\right)\right)\right]\vec{i}+\left[\Delta t\left|\frac{\vec{U}_+ +\vec{U}_-}{2}-\vec{U}_e\right|\frac{m_{i+1}-m_{i-1}}{2}\right]\vec{j}$$
$$\vec{X}_{ir}=\vec{X}_{te}+\left(\vec{U}_e+\frac{\vec{U}_+ +\vec{U}_-}{2}\right)\frac{\Delta t}{2}$$

The absolute vorticity $\left(\vec{w}=\overrightarrow{rot}\vec{U}_a\right)$ on each particle has to satisfy the Helmholtz equation written in the moving relative frame:

$$\frac{D\vec{X}_r}{Dt}=\vec{U}_a-\vec{U}_e;\ \frac{D\vec{w}}{Dt}=-\left(\vec{w}\cdot\overrightarrow{\overrightarrow{grad}}\right)\vec{U}_a+\left(\vec{\Phi}\wedge\vec{w}\right) \qquad (17)$$

where $\frac{D}{Dt}=\frac{\partial}{\partial t}+\left(\vec{U}_r\cdot\overrightarrow{\overrightarrow{grad}}\right)$ is the convective derivative in the moving relative frame of reference.

Coupling method

The coupling technique is the determination of the balance sailing boat position in navigation up the wind when it is submitted to the hydrodynamic forces (due to the hull) and the aerodynamic forces (due to the sails).

Forces and moments on a sailing boat

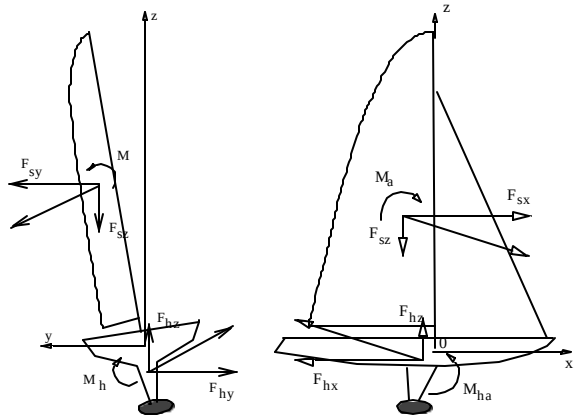

Fig. 2 Sketch of the aerodynamic and hydrodynamic forces on a sailing boat

We are going to define the aerodynamic forces on the sails and the hydrodynamic forces on the hull.
· F_{sx}, F_{sy}, F_{sz} are the three components of the aerodynamic forces in directions *x,y,z*. These forces are responsible of the three moments associated M_t (responsible of the trim angle, due to F_{sx} and F_{sz}), M_h (responsible of the heel angle, due to F_{sy} and F_{sz}) and M_y (responsible of the yaw angle, due to F_{sx} and F_{sy}) with respect to the same axis, x, y and z.
· F_{hx}, F_{hy}, F_{hz} are the three components of the hydrodynamic forces, also responsible of the three moments associated, M_{ht}, M_{hh} and M_{hy}.

The steady stability of a sailing boat required that the 6 following equations be satisfied:

$$\begin{cases}F_{sx}=F_{hx};\ F_{sy}=F_{hy};\ F_{sz}=F_{hz}\\ M_t=M_{ht};\ M_h=M_{hh};\ M_y=M_{hy}\end{cases}$$

Although this problem is a steady one, it is a complex one. That is why we are going to do some simplifications.

1. To face to the force F_{sz}, the hull has to produce a vertical force, due to hydrostatic (Archimedes) and dynamic pressure. If the variation of the submerged volume of the hull is small, we can consider that $F_{sz}=F_{hz}$.
2. If boat is well balanced, the forces induced by the rudder are weak and so, the moment producing the turning of the boat too. We can deduce that $M_y=M_{hy.}$
3. The moment M_t responsible of the trim modification can be balanced by a hydrodynamic force on the hull or by the displacement of a member of the crew. So we assume that $M_t=M_{ht}$.
4. In this simulation, we assume that the heel angle can be neglected, so that $M_h \cong M_{hh} \cong 0$.

Then, we have to solve the system:

$$F_{sx} = F_{hx}\,; F_{sy} = F_{hy}$$

These 2 equations enable to obtain an estimation of the boat speed and drift angle. Hydrodynamic forces are calculated by the hydrodynamic code described previously. From the numerical forces expressed in function of velocity and drift angle, a continuous interpolation surface is built using an interpolation function. We then determine the hydrodynamic forces from the knowledge of the boat speed and drift angle. This function are included in the aerodynamic code (Charvet, 1992, Hauville, 1996) where at each time step, the aerodynamic forces induced by the sails are estimated. The process is iterative and enables when the convergence is reached, to obtain an equilibrium point of the boat (speed, drift angle, apparent wind angle and wind speed).

Description of the coupling method

The method is based on the resolution of the following Newton's system:

$$\begin{cases} M A_{bx} = F_{sx} - F_{hx} \ (a) \\ M A_{by} = F_{sy} - F_{hy} \ (b) \end{cases} \qquad (18)$$

where A_{bx} and A_{by} are the x and y-component of the acceleration and M is the boat mass in navigation (with crew and equipment). By integration, the boat speed, the new apparent wind speed and wind angle are estimated. About 50 iterations are required to obtain an equilibrium state ($A_{bx} \cong A_{by} \cong 0$). Then after obtaining the equilibrium position, the speed and drift angle of the boat are calculated. Initially, the boat is assumed to be at rest and the sail in an uniform flow. After some few iterations, time required for the formation of the starting vortex and its departure from the sail trailing edge, the boat is able to move without drift angle. The Newton equation in direction x is then solved (Eq. 18a).

VALIDATION OF THE NUMERICAL CALCULATIONS

Steady flow and sea-keeping computations

Figure 3 plots the wave resistance $C_w = R_x/(\rho g c^3)$ of a submerged ellipsoid with b and a as axis, already studied by Farell (1973), versus the Froude number defined by $F = U/(\sqrt{gc})$, where $c = \sqrt{a^2 - b^2}$. Figure 3a is for lower Froude numbers and Fig. 3b for higher ones. The ratio of the body axis is a/b=0.5 and the depth of immersion is given by $h = 0.5c$. Results are in good agreement with the semi analytical method of Farell (1973), and with two other potential based panel method with Kelvin singularities (Ponizy *et al*., 1998, Kim, 1992) as soon as the number of panels is about 1000, even for low values of the Froude number. The agreement is also good for boats as Wigley hull or Antiope.

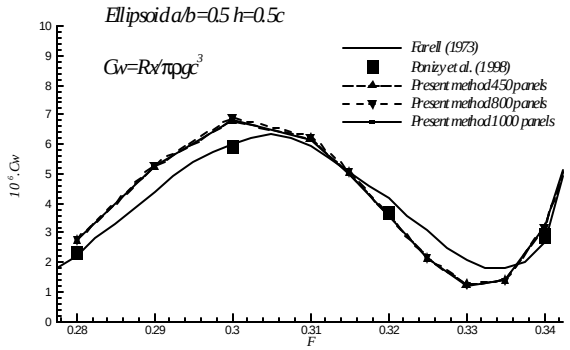

a) Low Froude numbers

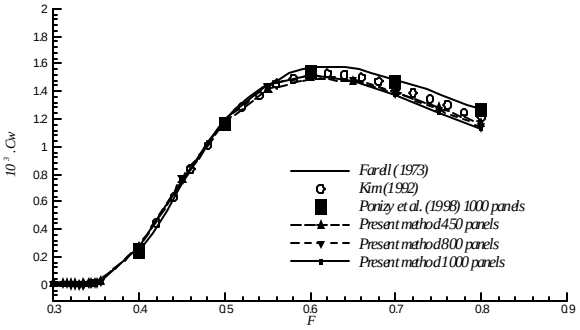

b) Higher Froude numbers

Fig. 3 Steady wave resistance coefficient versus the Froude number on a submerged ellipsoid

Figure 4 plots the results of the added-mass and damping coefficients versus the reduced frequency $w_c = w\sqrt{L/g}$ for the surface-piercing ellipsoid (axis ratio 8:1), already studied by Du *et al. (1999)*, at Froude number F=0.2. The number of panels is 480. The results of the present method (solid line) is in good agreement with the ones of Du *et al*. (1999).

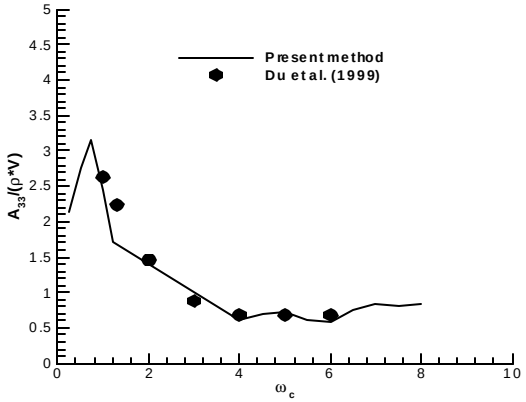

a) Added-mass

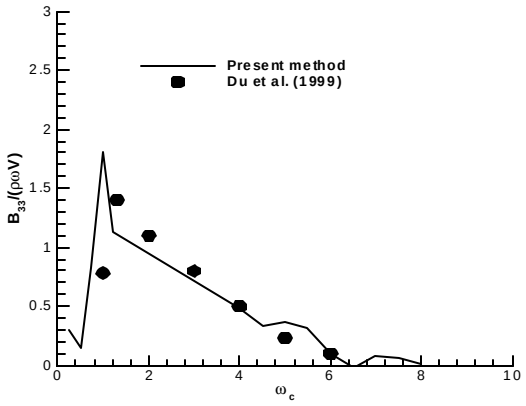

b) Damping

Fig. 4 Unsteady coefficients on a surface-piercing ellipsoid versus the reduced frequency (F=0.2; N=480)

Aerodynamics of sails

Although the numerical method has already been tested for various aerodynamic problems, a set of validation tests has been performed for sails in order to gain confidence in the ability of the model to describe such flows. The results have been reported in Charvet (1992) and are summarised in table 1. The agreement is quite good for the lift coefficient and acceptable for the drag one considering the assumptions made and the uncertainties on the true shapes of the jibs.

Table 1 Comparison between computed and measured drag and lift coefficients on various jibs

	Jib 1			Jib 2			Jib 3		
	11°	15°	19°	11°	15°	19°	11°	15°	19°
Test									
C_l	0.88	1.21	1.44	0.75	1.10	1.37	1.07	1.33	1.48
C_d	0.095	0.14	0.22	0.06 6	0.11	0.18	0.11	0.17	0.26
Com									
C_l	0.88	1.14	1.37	0.80	1.17	1.32	1.08	1.34	1.55
C_d	0.053	0.09	0.13	0.05	0.10	0.13	0.08	0.12	0.16

	Jib 4			Jib 5		
	11°	15°	19°	11°	15°	19°
Tests						
C_l	1.08	1.37	1.54	0.83	1.19	1.41
C_d	0.13	0.18	0.25	0.08	0.13	0.21
Comp.						
C_l	1.08	1.38	1.55	0.82		1.49
C_d	0.095	0.13	0.17	0.05	0.07	0.14

RESULTS OF THE COUPLING METHOD

Description of the case under study

The First Class 8 is a 8m long ship. This boat has been designed by the architects Jean-Marie Finot and Jacques Fauroux. We will present here the hull and the sails of this sailing boat. The hull is composed of 960 panels; the water plane length is 6.65m and the maximum draft is 1.92m. The rig is made of a fractional mast, a genoa and a main sail. The opening angle of the chord (defined as the line joining the tack point and the clew one) of the genoa with the boat axis is 12°. The luff length of the main sail is 10m, the one of the foot is 3.4m. The rig with the genoa and the main sail is shown on Fig. 5a. The opening angle of the boom with the boat axis is 4°. The repartition of the volume, the twist angle, the roach and the whole set of characteristics of the sails have been given by the sail maker Bernard Mallaret (Delta Voile Company). Figure 5b shows a sketch of the wake of the rig.

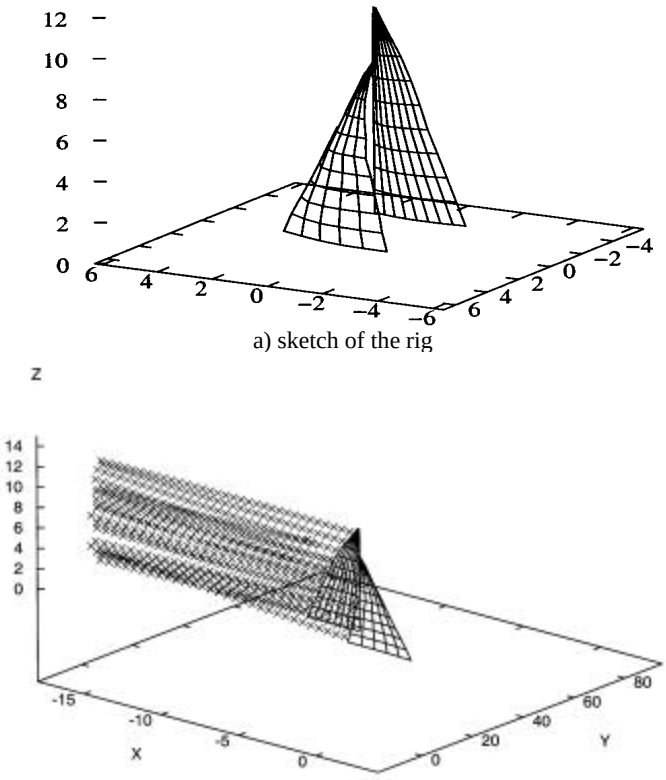

a) sketch of the rig

b) representation of the wake

Fig. 5 Sketch of the sails and of the wake after 172 iterations (non dimensional time 103.2), apparent wind angle 23°

Hydrodynamic results on hull

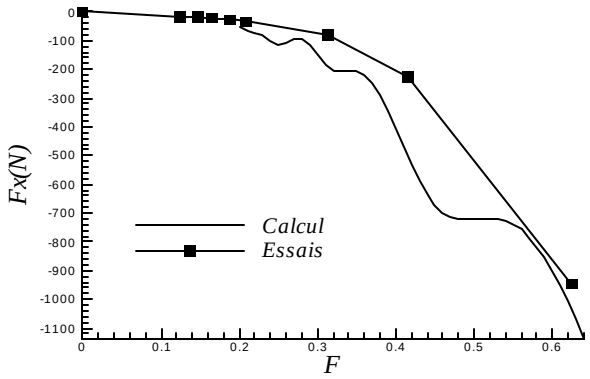

Fig. 6 Steady wave resistance versus the Froude number on the First Class 8 hull